The Palladium Potential of the Skaergaard Intrusion, South-East Greenland

Troels F. D. Nielsen

G E U S

The Palladium Potential of the Skaergaard Intrusion, South-East Greenland

Troels F. D. Nielsen

Contents

Abstract

The Palaeogene Skaergaard intrusion at 68 degree north on the rifted North Atlantic margin of East Greenland is a tabular or box-like body of gabbro. The original volume was close to 300 cubic kilometres. Approximately half of the volume is preserved. The body was 11 km N-S, 7-8 km E-W and in the order of 4 km deep. Post solidification block rotation has given the intrusion a southerly dip of 15 to 20 degree.

Subdivision of the gabbros on basis of liquidus parageneses allow the study of the internal structure. Cooling from floor, walls and roof of the intrusion resulted in an onion type internal structure with the most evolved liquid concentrated in the upper and central part of the intrusion. The internal structure is mapped out using depth control from exploration drill cores.

Mass balances for the intrusion suggests the parental melt to be an evolved tholeiitic basalt (Mg# = 0.45) comparable to contemporaneous tholeiitic flood basalts. The revised mass proportions for the major zones within the tabular body corroborate with petrogenetically estimated mass proportions.

The Au-Pd deposit is continues and stratabound. It consists of a series of mineralised levels defined by palladium. The levels can be correlated to the finest detail from core to core. Gabbros between defined Pd-levels are poor or void of Au and PGM. The lowermost level (Pd5) is in all investigated cores situated in the lower half of the so called "L zero" leuco-gabbro of the macrorythmic "Triple Group" gabbro sequence in top Middle Zone. Pd5 is found in all cores and chip lines through out the intrusion. The Pd4 level above is found all over except for the chip lines most distant from the supposed centre of the intrusion. The Pd3 level is found more centrally and the Pd2 and Pd1 levels only in the central parts. In each level the platinum/palladium ratio decreases away from the centre of the intrusion.

Gold is concentrated in the uppermost Pd-level. At the margin of the intrusion it is concentrated in Pd5 and/or Pd4, in the more central parts in Pd3 and or Pd2 and in the central parts in Pd1 or in mineralised Au2 to Au4 levels above. As a whole the structure is seen as a set of plates defined by palladium. The plates are separated by Au and PGM poor gabbro. The plates have decreasing size up through the deposit. The origin of the this type of structure is not clear, but the architecture and the petrography suggest magmatic control.

The Pd5 level is up to 7 meters thick at 1 g/t Pd cut of. It contains a variety of Pd, Pt and Au phases related to or in sulphide droplets and as individual crystals in intercumulus parageneses or in rims of cumulus phases. The textural observations suggests the mineralisation to have formed during the crystallisation of the intercumulus melt.

The mineralogy of the main palladium part of the deposit is complex. Towards the margins the dominant precious metal phases are CuPd-alloys and Pd-arsenites. In the central parts of the intrusion CuPd-alloys dominate.

The potential of the deposit is estimated assuming the drill core data to be representative and that average concentrations can be calculated from the data, despite significant distances between drill cores. The systematics and strict control suggest that this is permissible.

The potential resource in the Pd5-level is in the drilled parts of the intrusion 250-300 million tons with 1,9 g/t palladium and 2.11 g/t combined Pt, Pd and Au over an area of 19 square km and an average width of 4.7 m. Higher concentration can be found in parts of the deposit and/or over a decreased width of 2 m. The total content of PGM+Au metal in the Pd5-level is in the order of 1000 metric tons. In the entire deposit probably more than 1500 metric tons.

Introduction

Since the gold exploration and drilling campaigns in the Skaergaard intrusion between 1986 and 1990 palladium has become a most important PGE in the production of auto catalysts and is in high demand. Two thirds of the palladium on the world market originates from Russia. Through parts of 1999 and year 2000 supplies from Russia to the world market are doubted and the result is that spot palladium reached all time highs above 800 US $/oz since December, 2000. The predicted palladium price for the coming years is believed to remain high due to a continued and expanding demand for palladium for auto catalysts and a possible shortage in the supply of palladium. In view of these problems the development of alternative sources for palladium is attractive.

The Skaergaard intrusion contains beside gold significant palladium and has the potential for a world class deposit. Resolution of the structure of the deposit allows evaluation of the potential of the deposit.

The Skaergaard intrusion

Location

The Skaergaard intrusion is located at tide water, 68°N on the east coast of Greenland (Fig. 1). The transit time from Northwest Iceland is app. 20 hours by sea and app. 1:45 hour by air. A dirt strip is located ca. 12 km east of the intrusion. Although located in the Arctic the intrusion is in general not affected by permafrost at sea level. The geothermal gradient in the intrusion has been measured to 20-25°C/km (C.K. Brooks, pers. comm., 1995).
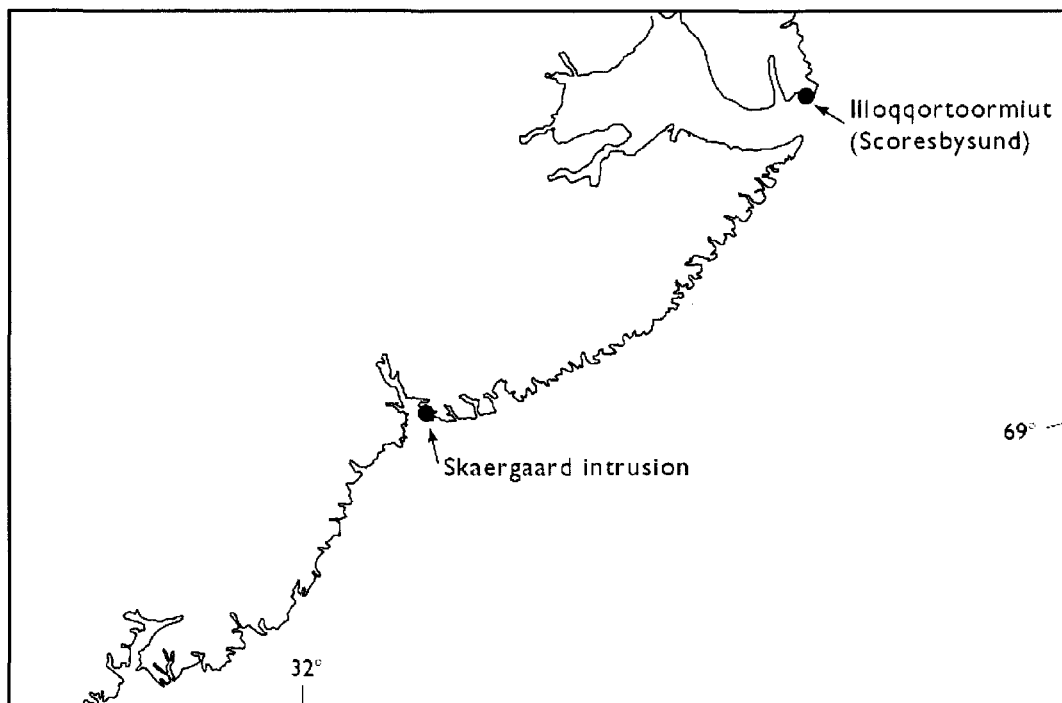
Figure 1. *Location of the Skaergaard intrusion in East Greenland.*

Geological setting

The Skaergaard intrusion was first investigated in the 1930's and the classic description of the intrusion by Wager & Deer (1939) made the Skaergaard intrusion (Fig. 2) an unparalleled type locality and natural laboratory for the study of crystallisation of basaltic magma in crustal magma chambers. No other intrusion has received so much academic attention.

Skaergaard was emplaced 55 million years ago during the opening of the North Atlantic (Hirschman *et al.*, 1998). The current understanding suggest that the intrusion was emplaced in the tectonic and magmatic Rifted Volcanic Margin of East Greenland between Cretaceous to Tertiary sediments and the *c.* 3 km of the flood basalt had formed at the time of the emplacement of the intrusion. Flood basalt magmatism continued after the em-

placement of the intrusion and an additional 5-7 km thick sequence was deposited in the region over a period of 1-2 million years. The continental margin continued to be a region of magmatic and tectonic activity until c. 15 M.a. ago (Storey *et al.*, 1996).
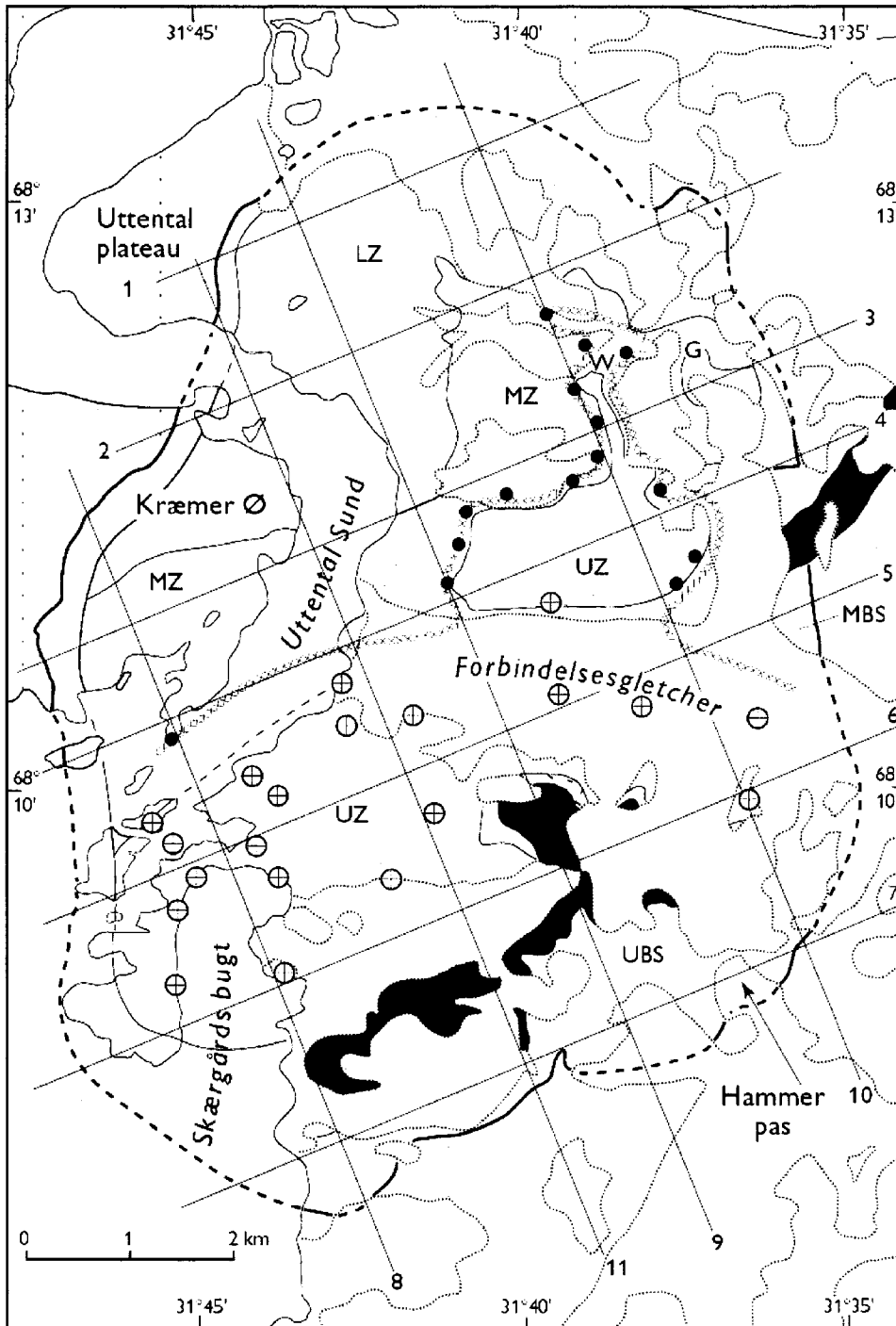
Figure 2. *Skaergaard overview map based on McBirney (1989a). Drill sites are indicated by crosses in circles, chip line profiles by dots and the Platinova reefs by line of crosses. Constructed sections numbered from 1 to 11. LZ: Lower Zone; MZ: Middle Zone; UZ: Upper Zone and UBS: Upper Border Group.*

The classic Skaergaard intrusion

The geological map of the intrusion (Fig. 2) by Wager & Deer (1939) has only received minor revision. The most up to date topographic and geological maps of the intrusion are published by Geodætisk Institut (1975) and McBirney (1989a), respectively. The terrain is alpine with peaks up to 1000 - 1200 metres in two massifs south and north of the glacier "Forbindelsesgletscher" (Fig. 2). Uttental Sund separates the exposures on Kraemer Ø from the main part of the intrusion. Many of the classic studies of the gabbros of the intrusion have over decades been conducted in the very well exposed and accessible areas on Kraemer Ø, along Uttental Sund, on Uttental Plateau and on Skaergaardhalvø (Fig. 2). It is here that most of the classic textbook localities of magmatic layering, trough bands, etc. are located (e. g., Wager & Brown, 1968).

In plan view the intrusion is an oval magmatic body, up to 7 – 8 km E-W and app. 11 km N-S (Fig. 2). To the south and east the country rocks comprise Cretaceous to Tertiary sediments and the lower part of the basalt province (Wager & Deer, 1939, Nielsen *et al.* 1981) and to the west and north the Precambrian basement of amphibolite facies granitoids and supracrustals. The intrusion dips 10-20°S as result of post-emplacement tectonics.

The shape of the intrusion has received significant attention and three main models have been proposed. Wager & Deer (1939) originally proposed a funnel-shaped intrusion of which only the upper 40 % of the volume is exposed (Fig. 3a). Norton *et al.* (1984) used gravimetric data and modelled the intrusion as a lacolith type magma chamber developed from a sill and supplied from two channels or roots below the centre of the intrusion (Fig. 3b). The most recent interpretation of the magma chamber was presented by Irvine (1992) who noted the very steep orientation of the margins of the intrusion and resolved that several of the contacts of the intrusion probably were fault controlled (Fig. 3c). This is of major importance for the interpretation of the emplacement dynamics and volume relations in the intrusion and forms the basis for the modeling of the intrusion and its mineralisation.

The gabbros of the intrusion are divided into 3 main structural units (Wager & Deer, 1939). The Layered Series (LS) accumulated up from the floor of the intrusion, the marginal Border Group (MBG) crystallised along the walls of the magma chamber and the Upper Border Group (UBG) accumulated down from the roof of the intrusion (Fig. 4). Upper Border Group and the Layered Series meet at the Sandwich Horizon (SH) that contains the most evolved compositions of the intrusion. This description assumes that the gabbro body crystallised-from all the melt originally emplaced into the magma chamber and that no evolved liquid was extruded from the magma chamber, a view held by most investigators.

This view was challenged by Hunter & Sparks (1987), who based on a comparison with the development of Icelandic tholeiite lavas and petrogenetic modeling argued: (1) that a late differentiated silica-rich melt had been lost from the intrusion and (2) that the latest formed gabbros do not represent the bulk crystallisation products of the most evolved liquid, but cumulates from the granophyric magma that had been expelled from the magma chamber.
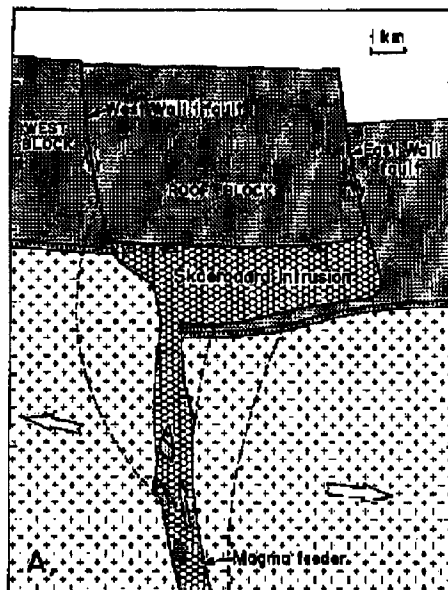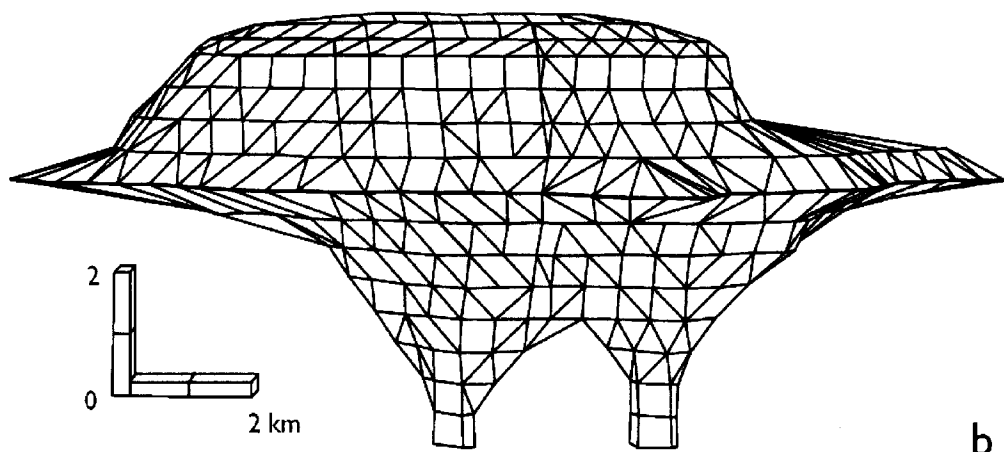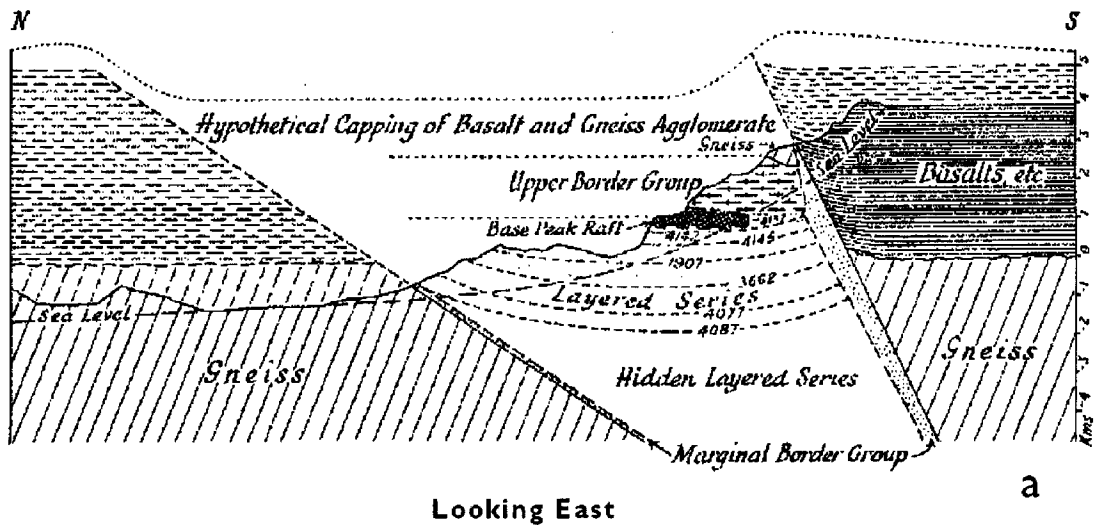
Figure 3. *Shape of the intrusion: (a) from Wager & Deer (1939); (b) geophysical model from Norton et al. (1984) and (c) from Irvine (1992).*

The layered Series: LS is subdivided into four zones (Fig. 4). The lowest zone – Hidden Zone (HZ) - is the cumulates of the intrusion that are not exposed. The exposed part of the LS is subdivided into three zones based on the cumulus parageneses. The lowest exposed zone – Lower Zone (LZ) - is subdivided into three sub-zones: LZa, LZb and LZc on the basis of liquidus parageneses. LZa has plagioclase and olivine on liquidus, LZb has plagioclase and olivine plus clinopyroxene on liquidus and LZc has plagioclase, olivine and clinopyroxene plus magnetite and ilmenite on liquidus. Middle Zone (MZ) that separates Lower Zone (LZ) from Upper Zone (UZ) is generally void of liquidus olivine and has the liquidus assemblage plagioclase, clinopyroxene, low-Ca pyroxene and magnetite and ilmenite.
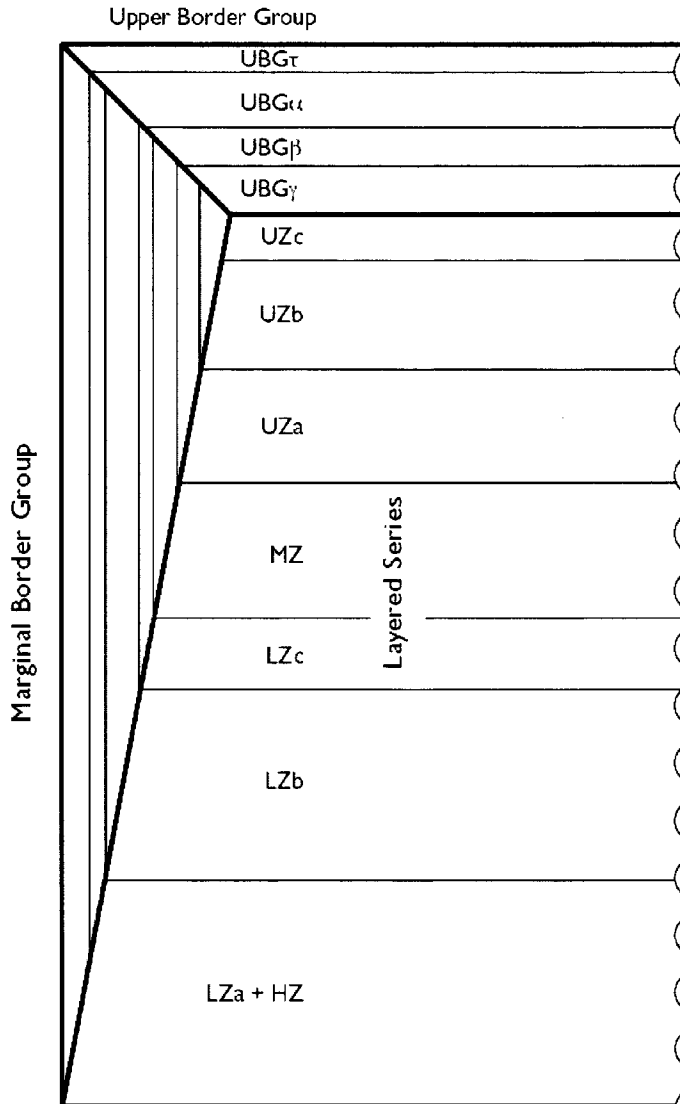
Figure 4. *Schematic illustration of the subdivisions of the intrusion (after McBirney, 1989a).*

The re-appearance of olivine as a liquidus phase defines the boundary between MZ and UZ. UZ is divided into three sub-zones on the basis of liquidus parageneses. UZa has plagioclase, olivine, clinopyroxene and magnetite on liquidus. The boundary to UZb is marked by the incoming of apatite as a liquidus phase and the boundary to UZc is marked by the incoming of ferro-bustamite as a liquidus phase.

All of the phase boundaries are mapped out all over the intrusion and equivalent zones are mapped out in both MBG and UBG. Most authors agree that LS, MBG and UBG all followed parallel trends of crystallisation and fractionation and for the present purposed the development in LS is taken to represent the development of the entire magma in the intrusion. Some important systematic differences are, however, observed between the LS, MBG and the UBG, but they are not believed to affect the general models presented below.

From the lowest exposures to SH where the LS meets UBG all the liquidus phases show systematic developments in broad agreement with experimental systems. Plagioclase evolves from anorthite-rich (An_{70}) to albite-rich compositions and all MgO and FeO-bearing silicate phases have decreasing Mg# to almost pure Fe-endmembers at SH. The phase layering and the systematic cryptic variation in the chemistry of the liquidus phases is the basis for the interpretation of the gabbros as the cumulates of an undisturbed, cooling, and fractionating basaltic magma (Wager & Deer, 1939).

A revised model for the Skaergaard intrusion

The shape of the intrusion and its internal structure can be reconstructed based on and inspired by the concepts of Irvine (1992) and the information obtained from exploration drill cores and observations along the chilled margins of the intrusion. The understanding of the structure of the intrusion is in part a requirement for the evaluation of the potential of the Au-PGM deposit in the intrusion. Based on the reconstruction and the estimates of the bulk compositions of all zones and sub-zones in the intrusion, a new and more well constrained mass-balance can be made for the intrusion.

The shape of the intrusion

A chilled margin is exposed along approximately half of the periphery of the intrusion. For simplicity the margin is here divided into four parts: the western, the northern, the eastern and the southern margin. The western and eastern margins are - where they can be studied and as noted by Irvine (1992) - generally steep and they are both accepted to be sub-vertical (see also McBirney, 1989a). The southern margin is more complex – and as shown in cross sections of Irvine (1992) and Irvine et al. (1998) composed of a mainly sub-vertical southern wall and a restricted exposure of the shallow S-dipping roof contact. The steep northern contact is mostly not exposed, except in a small exposure at the NW and NE corner of the intrusion. The roof contact at the southern margin separates the gabbros of UBG from the overlying lava successions.

The eastern and southern contacts are all sub-vertical and by analogy to the interpretation of the western margin (Irvine 1992, Irvine et al. 1998) all these margins are suggested to be sub-vertical, fault controlled walls of the magma chamber. The gabbros near the northern exposures dip 10-20 degree S and similar to the roof contact at the southern margin. The roof contact – although the exposures are limited – appears in general to follow bedding in the sedimentary and volcanic host rocks. By analogy to abundant sill-like gabbroic bodies in the region it is suggested that the shape of the intrusion is determined by fault controlled walls and a floor and roof determined by bedding planes in the Palaeogene hosts.

Based on these observations and assumptions a tabular or box-like magma chamber (Nielsen & Andersen 1996) is suggested (Fig. 5). The box would be approximately 7.5 km E-W, 11 km N-S and up to 4 km deep – as modelled from cross sections (see below). Due to post-emplacement block rotation the box has been faulted and tipped and bend to the SSE. Due to the inherent limitation in the modeling the shape of the intrusion is simplified to a major southern box 7.7 x 9 x 3.8 km and a smaller northern box of 2 x 5.3 x 3.4 km.
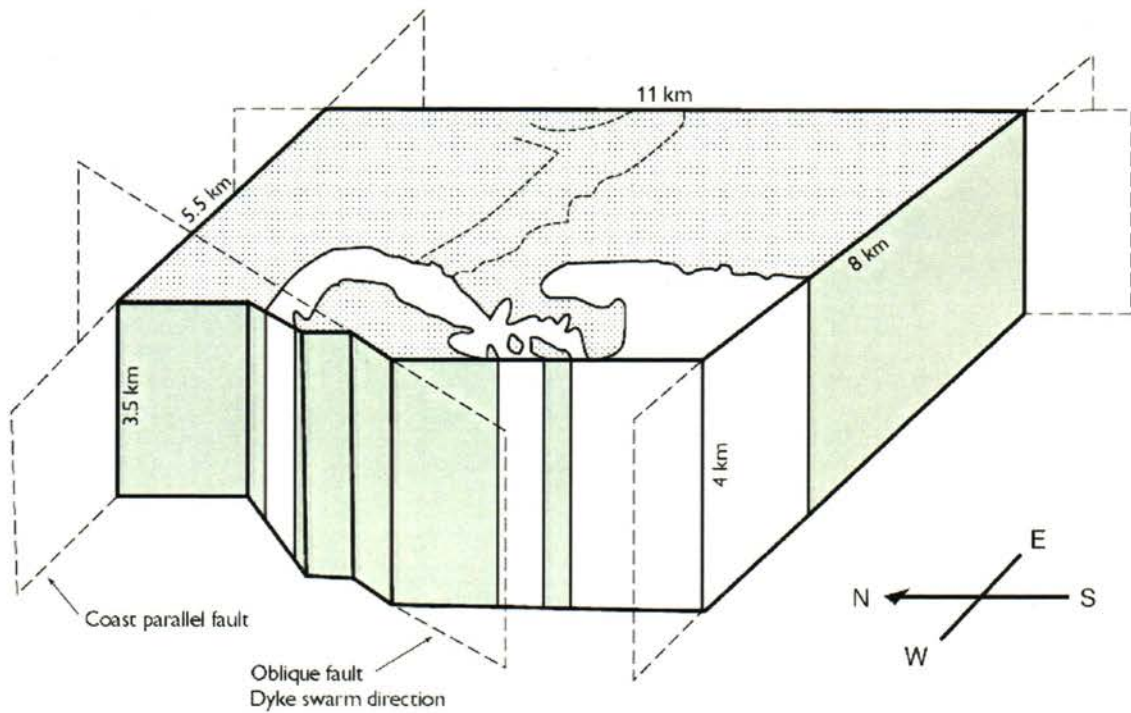
Figure 5. *Box model from Nielsen & Andersen (1996).*

Shape compared to geophysical models

The box model for the intrusion is in figure 6 superimposed on the geophysical model of the magma chamber by Norton *et al.* (1984). The box model overshoots the geophysical model at the intersection between roof, floor and walls, but the excess volumes (in red) are either not preserved due to erosion or too small and within the uncertainty of the geophysical modeling. The box model does not include the sill-like extensions (in green) of the magma chamber modelled by Norton *et al.* (1984). The sill-like extension to the north of the intrusion is purely model driven. The sill-like extension could not have contributed to the gravimetric anomaly on which the geophysical model is based. Norton *et al.*. (1984) suggests that the sill-like extensions at the southern margin could result from anomalies produced by exposed pre-Skaergaard sills and no Skaergaard related sill extensions can be substantiated south of the exposures of the intrusion. Along the western and eastern margins no sills as the ones suggested in the model of Norton *et al.* (1984) can be observed and all sill extensions can with good reason be excluded. The remaining main part of the geophysical model is contained in the two roots of the intrusion (in blue). It can not be excluded that such masses of gabbro do occur below the Skaergaard intrusion, but there is no evidence to exclude that these masses represent pre-Skaergaard material, e. g., related to the Mikis Fjord Macro Dikes that project into the intrusion and which by all likelihood pre-dates the intrusion or that they represent other intrusive mafic material. Alternatively, the revision of the density distribution in the intrusion may question the existence of such roots.
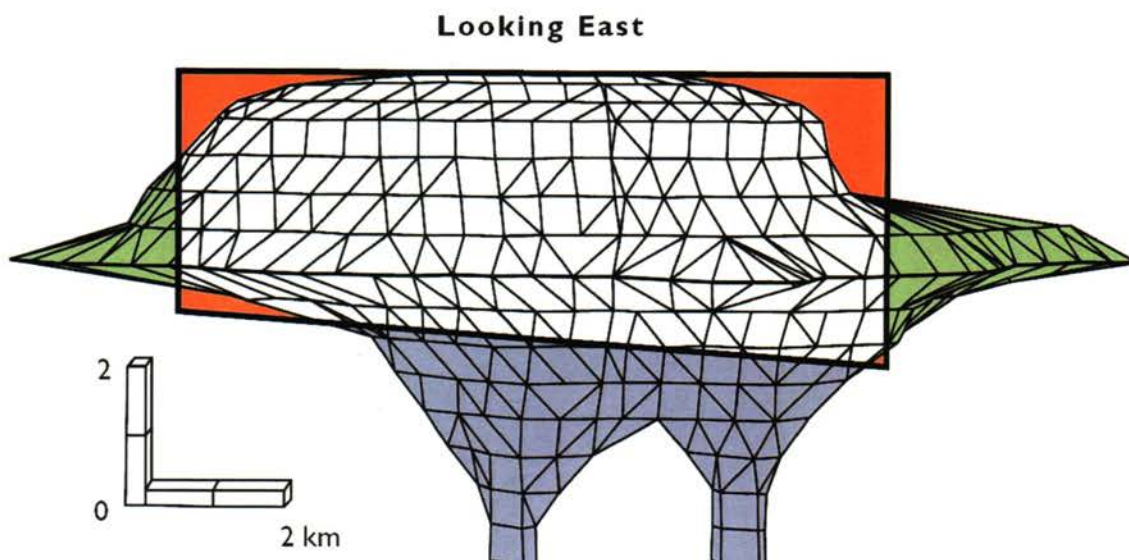
Figure 6. *Box model (Fig. 5) overlain on geophysical model (Fig. 3b).*

It is concluded that the geophysical model does not prove the box model to be correct, but it is argued that the geophysical model does not contradict the box model suggested in this report.

The internal structure

Wager and Deer (1939) visualised the intrusion as a funnel-shaped structure with originally near-horizontal internal boundaries in LS and UBG and sub-vertical contacts in MBG. This view has remained essentially unchanged throughout the years, but is challenged by the observations in exploration drill cores. In the cross sections (Fig. 7) the boundaries between zones and sub-zones - as identified in exposures and in drill cores - form an onion type structure. Instead of a systematic near-planar accumulation on the floor, down from the roof and in from the walls of the magma chamber the accumulation appears to result in an onion type structure due to contemporaneous crystallisation and accumulation into the magma chamber from the walls, the floor and the roof.

Not all boundaries can be followed in the drill cores, but the upper boundary of MZ that is identified in most drill cores and is well established in surface exposures shows a sagging in the order of 700 m in the centre of the intrusion (Figs 7a and 7b). The sagging is equivalent to app. 10 % to the width of the intrusion. This combined with contemporaneous crystallisation of equivalent zones of gabbros under roof of the intrusion in UBG and along the walls of the intrusion in MBG suggest that correlated zones in LS, MBG and UBG together form shells of decreasing size towards a final late crystallising volume in the upper central part of the magma chamber (Fig. 7).
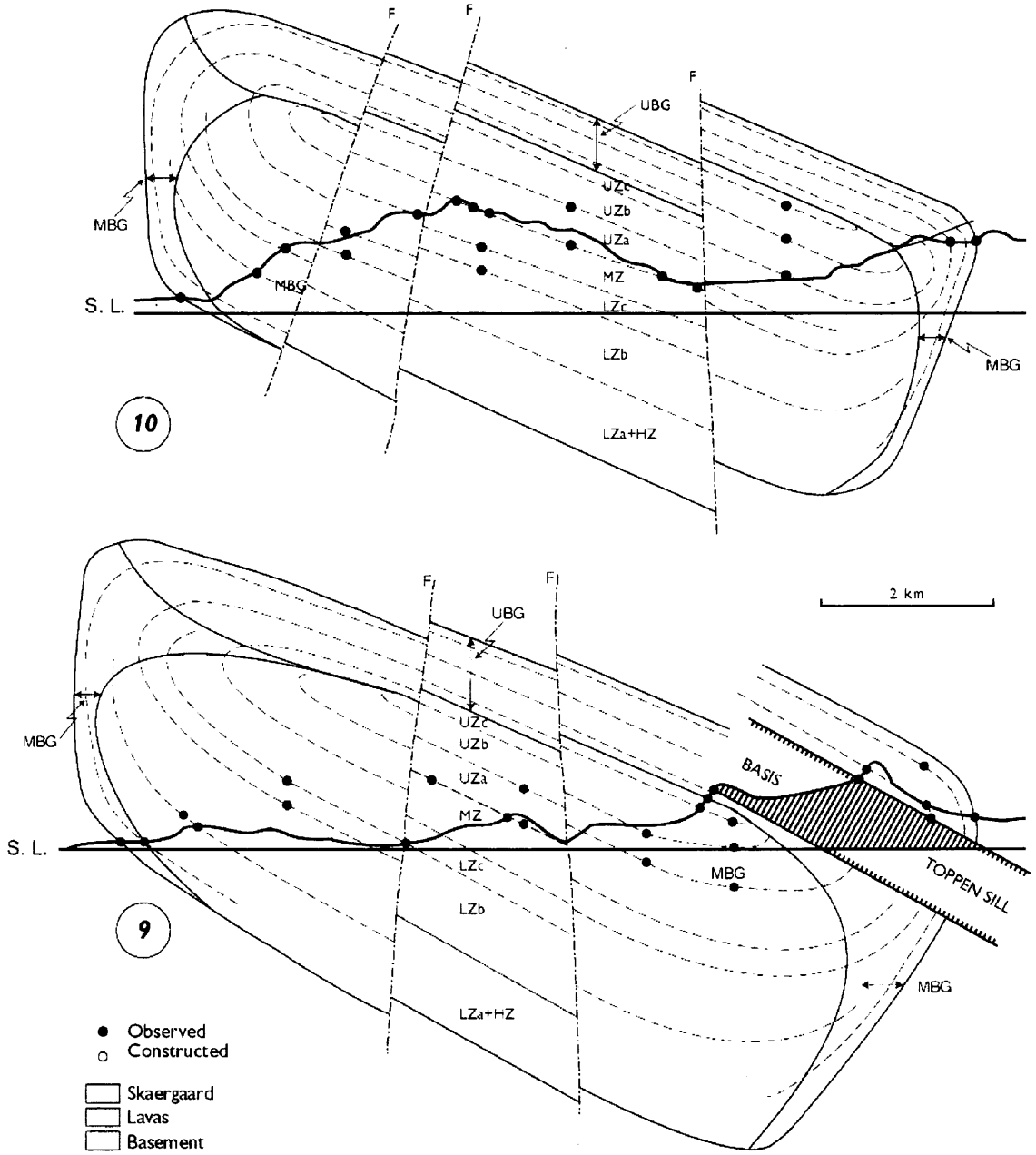
Figure 7a. *Reconstructed N-S section. See location in figure 2.*
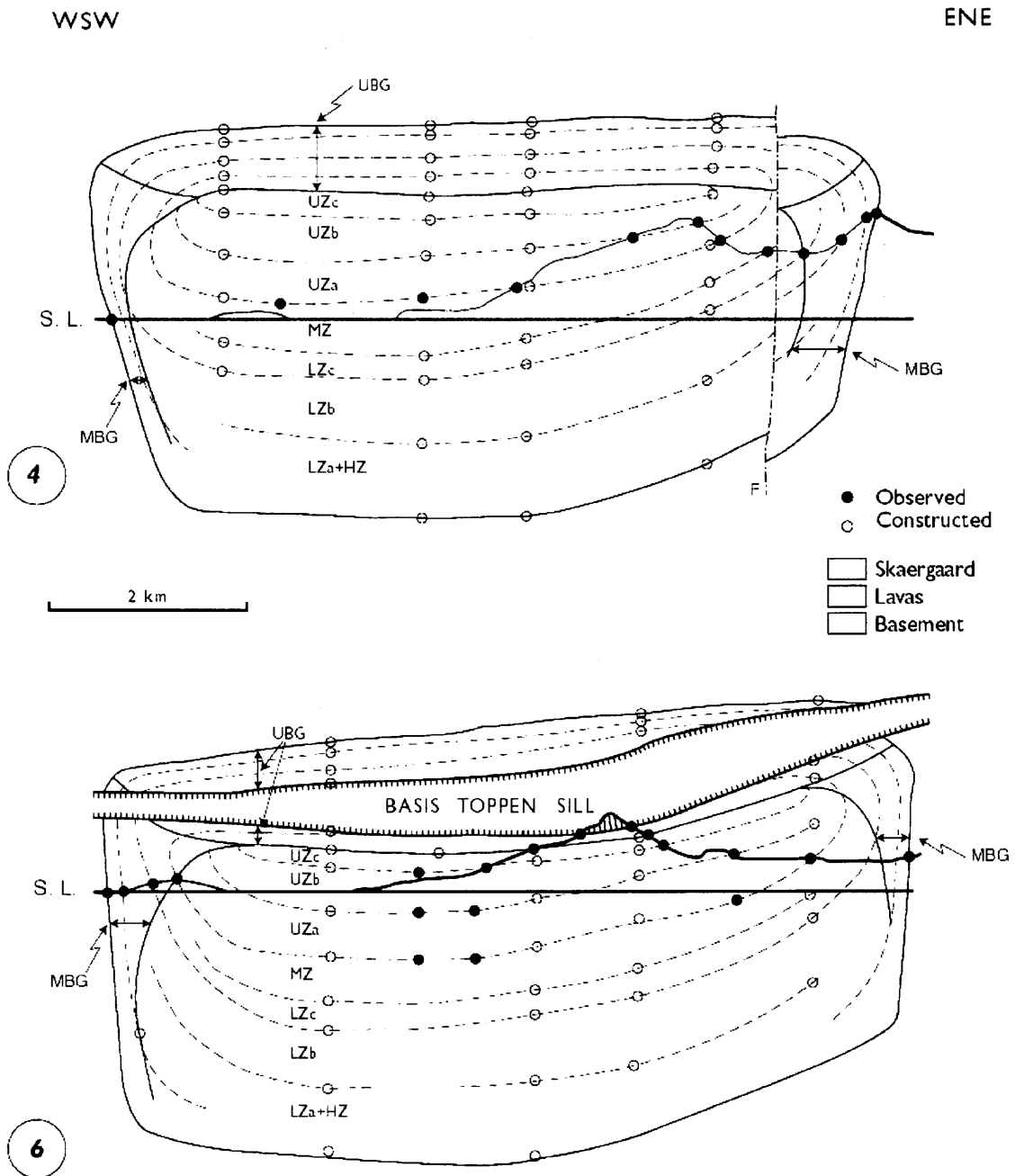
Figure 7b. *Reconstructed E-W section. See location in figure 2.*

UBG is defined as the gabbros deposited down from the roof to the Sandwich horizon through the last crystallising sub-zone (UZc). The MBG is defined as the volume between walls of the magma chamber and a surface from the intersection between walls and floor, through the intersections between the vertical tangents to the shells of the individual zones and sub-zones and to the intersection between roof and walls (Fig. 4).

In the cross sections all the zones and sub-zones are modelled based on the assumptions: (1) that all boundaries are co-planar with the mapped MZ-UZ boundary and (2) that the

boundaries and the phase layering is determined by the temperature of the melt at the crystallisation front, which accordingly must have been smooth. In some sections faults have to be modelled and in most cases such faults are observed in surface exposures, but the resolution in the modeling does not allow a constrained correlation between modelled and observed faults. The faulting is related to the post-solidification rotation of fault blocks in the Volcanic Rifted Margin.

Volume proportions

Based on eleven cross sections in an WSW-ENE and NNW-SSE grid (Fig. 2, 1-11) the volumes of the individual series, zones and sub-zones of the layered series, and of the entire magma chamber can be estimated (Table 1). The total original volume based on the box model in figures 5 is calculated to $c.$ 300 km^3. The volumes of MBG and UBG are estimated in the cross sections (Fig. 7a and 7b) and calculated to $c.$ 50 km^3 and $c.$ 42 km^3, respectively. The volumes of UBG and MBG were calculated assuming average thickness of MBG of 350 m and of UBG of 600 m. This leaves $c.$ 200 km^3 for the LS.

The volume of each zone in LS has been estimated from the average height, width and length in the cross sections (Fig. 7). The sum of the volumes of sub-zones in LS, MBG and UBG is $c.$ 300 km^3. The volumes of zones and sub-zones in MBG and UBG have been calculated assuming volumes of zones and sub-zones in MBG and UBG to be equivalent to correlated zones and sub-zones in LS.

The most notable result of the volume modeling is that the volume proportion of UZ in LS is relatively small ($c.$ 20 %) and that the model suggest a large volume of HZ plus LZ rocks ($c.$ 66 %) without assuming the extension of the magma chamber to any great depth as suggested in the funnel model (Fig. 3a). This corroborates with the geophysical model of Norton *et al.* (1984) and the geochemical constraints presented by Brooks (1968) and Maaløe (1974).

Mass proportions and bulk composition

The volume proportion can be transformed into mass proportions (Table 2) for the calculation of a bulk composition for the intrusion and mass balances for, e. g., precious metals hosted by the intrusion. McBirney (1989b) gives the average compositions and norms for the individual zones and sub-zones of the LS, MBG and UBG. The densities of all zones and sub-zones (Table 2) are calculated based on the normative mineral proportions and appropriate mineral densities extracted from Deer, Howie and Zussman (1964).

The bulk composition (Table 3) is calculated on the basis of the mass proportions and the average compositions for the individual zones and sub-zones (McBirney, 1989). Model compositions were calculated using bulk average compositions for individual zones and sub-zones and assuming 2% and alternatively 5 % melanogranophyre melt contained in gabbro pegmatites.

Table 1. *Volume calculation for the Skaergaard intrusion.*

		km	km	km	km	km	km	km³	km³	km³
Box volume										
Southern box	7.7 x 9 x 3.8	7,700	9,000	3,800					263,340	
Northern box	5.7 x 2 x 3.4	5,700	2,000	3,400					38,760	
Total volume										302,100	**302,100**

		km	km	km	km	km	km	km³	km³	km³
Volume of individual zones and subzones										
UBG:										
average thickness: 0.6	(8 x 9 x 0.6) + (5.5 x 2 x 0.6)	8,000	9,000	0,600	5,500	2,000	0,600		49,800	
reduction due to MBG									*8,325*	
Total UBG										41,475
MBG										
Average width: 0.35 km										
South wall:	(0,35*(3,4*7,7))+((0,75*(0,6*7,7))/2)	0,350	7,700	3,400	0,600	7,700	0,750	1,733	10,896	
West wall 1:	(3.2x9.0x0.35)+((0.6x9.0x0.75)/2)	0,350	9,000	3,200	0,600	9,000	0,750	2,025	12,105	
N-1 wall:	(2.9x2.0x0.35)+((0.6x2.0x0.75)/2)	0,350	2,000	2,900	0,600	2,000	0,750	0,450	2,480	
W-2 wall:	(2.9x2.0x0.35)+((0.6x2.0x0.75)/2)	0,350	2,000	2,900	0,600	2,000	0,750	0,450	2,480	
E-wall:	(3.3x11.0x0.35)+((0.6x11.0x0.75)/2)	0,350	11,000	3,300	0,600	11,000	0,750	2,475	15,180	
N-2 wall:	(2.8x5.3x0.35)+((0.6x5.3x0.75)/2)	0,350	5,300	2,800	0,600	5,300	0,750	1,193	6,387	
Total:								8,325		49,527

km²

LZa + HZ
Max. constructed thickness at N margin: 0.7 km.
An increase in thickness to the South suggests an
average thickness of 0.9 km. Area of LZa + HZ is calculated
to 83 km2

	0,900	*83,000*		74,700

LZb
Constructed thickness at N margin: 0.65 km:
An increase in thickness to the South suggests an
average thickness of 0.7 km.
Area calculated to: 72 km2

	0,700	*72,000*		50,400

LZc
Average thickness: 0.25 km
area: 62 km2

	0,250	*62,000*		15,500

MZ
Average thickness: 0.48 km
area: 59 km2

	0,480	*59,000*		28,320

UZa
Average thickness: 0.4 km
Area: 52 km2

	0,400	*52,000*		20,800

UZb
Average thickness: 0.4 km
Area: 42 km2

	0,400	*42,000*		16,800

UZc
Average thickness: 0.18 km
Area: 31 km2
includes part of UBG /0.9 km3 equ. to c. 0.03 km

	0,150	*31,000*		4,650

SUM OF INDIVIDUAL VOLUMES			302,172
AVERAGE THICKNESS	**3880**		

Table 2. *Densities and mass proportions (see text)*

Zone or subzone	volume %	density	proportions	mass proportion %
LZa	24,72	3,07	75,89	23,90
MBS LZa	5,93	3,12	18,50	5,83
UBS alpha 1	4,81	3,02	14,53	4,58
LZb	16,68	3,16	52,71	16,60
MBS LZb	4,00	3,09	12,36	3,89
UBS alpha	3,25	3,04	9,88	3,11
LZc	5,13	3,36	17,24	5,43
MBS LZc	1,23	3,27	4,02	1,27
UBS alpha 2	1,00	3,05	3,05	0,96
MZ	9,37	3,31	31,01	9,77
MBS MZ	2,25	3,26	7,34	2,31
UBS beta	1,82	3,17	5,77	1,82
UZa	6,88	3,33	22,91	7,22
MBS UZa	1,65	3,31	5,46	1,72
UBS-gamma 1	1,34	3,06	4,10	1,29
UZb	5,56	3,38	18,79	5,92
MBS UZb	1,33	3,00	3,99	1,26
UBS gamma 2	1,08	3,09	3,34	1,05
UZc	1,54	3,39	5,22	1,64
UBS gamma 3	0,43	3,29	1,41	0,45
SH	0,00	-	-	-
Bulk cumulates	**100,00**		**3,175**	**100,01**

The calculated bulk composition is a basaltic melt with *c.* 7 % MgO. The addition of grano-phyre melt mostly affects the SiO_2 and K_2O of the calculated bulk composition. The calculated P_2O_5 appears comparable to contemporaneous tholeiitic lavas in East Greenland plateau basalts. This indicates that the relative mass proportion of the apatite-bearing zones (UZb and UZc) is approximately correct and that the calculated mass proportions seems meaningful. Similarly, the K_2O, Na_2O and MnO concentrations compare with normal plateau basalt compositions and support that the estimated relative mass of evolved gab-bros in UZ is acceptable. Using stratigraphic height as equivalent to proportion of crystal-lised melt (Wager and Deer model) the average P_2O_5 would be 0.46 % and much higher than expected for tholeiitic melt compositions.

The iron content of calculated melt appears to be high even though the Mg# of 0.45 cor-roborates with the estimated Mg# of the melt in equilibrium with the most Fo-rich olivines of

the LS (P. Thy *et al.*, 1997). The FeO content is, however, determined by the weighted FeO-contents of the individual zones and sub-zones of the intrusion as estimated by McBirney (1989b). 35.5 % of the mass of LS is contained in LZa and HZ and the iron content of LZa and HZ has significant importance for the evaluation of the bulk FeO. All available samples of LZa originate from exposures close to the walls of the intrusion and sedimentary structures in the gabbros show that slumps of cumulus phases (olivine and plagioclase) descended along the walls and spread over the floor on the top of the accumulating gabbros (e. g., Irvine *et al.*, 1998). It is argued that the average cumulate composition of LZa in McBirney (1989) may well be biased and enriched in equilibrium cumulus phases. That the FeO content in LZa may not be trusted to represent the average LZa+HZ cumulate composition is supported by the modeling of Thy *et al.*, (1997) who model average cumulate compositions during crystallisation of LZa and HZ to contain 7-8 wt.% FeO relative to the average composition of McBirney (1989b) of LZa with 11-12 wt% FeO.

One approach in the search for a reasonable bulk model composition is to use the Mg# as a guide for the bulk MgO. Larsen *et al.* (1989) describe the plateau basalt in East Greenland N of 69°N and report that melt compositions with Mg# close to 0.45 have MgO bulk concentrations in the region 5.5 to 6 % MgO with equilibriun olivine and plagioclase with close to Fo68 and An70, respectively. Assuming a selective increase in these cumulus phases in the available LZa and HZ samples the modelled bulk composition can be recalculated into a bulk composition with 5.5 to 6 % MgO by the subtraction of *c.* 10% modelled cumulus paragenesis with 50% olivine and 50 % plagioclase. The resulting liquid composition shows very significant similarities with the high Ti lavas of the Giekie Formation (Table 3), which could well be contemporaneous with the Skaergaard intrusion.

The conclusion of the modeling is that the bulk composition of the intrusion is a tholeiitic basalt melt with less 7 % MgO that most likely compares with contemporaneous flood basalts (Larsen *et al.*, 1989). This could open for the possibility of more Au-PGM mineralisations related to the Palaeogene magmatism. Petrogenetically it is also an important conclusion that there is no compelling mass balance evidence for any significant loss of silica-rich magma from the intrusion.

Table 3. *Skargaard model melt and comparisons.*

Recalculated to 100% volatile free

	1	2	3	4	5	6	7	8	11	12	13
SiO2	47,73	47,28	48,17	47,70	48,03	48,86	48,85	48,96	48,68	48,98	48,94
TiO2	2,97	3,03	3,15	3,21	3,32	3,09	3,02	3,23	3,47	3,28	3,26
Al2O3	13,41	13,44	14,06	14,09	13,14	12,91	12,90	12,66	12,74	12,76	12,83
FeO*	15,61	15,71	15,01	15,12	15,80	15,24	15,17	15,69	15,36	15,52	15,20
MnO	0,23	0,23	0,24	0,24	0,25	0,23	0,24	0,24	0,23	0,33	0,32
MgO	7,02	7,22	5,67	5,89	5,97	5,80	5,99	5,60	5,72	5,58	5,74
CaO	9,85	10,01	10,38	10,56	10,18	10,71	11,03	10,45	10,44	10,34	10,37
Na2O	2,50	2,45	2,62	2,56	2,57	2,47	2,40	2,43	2,71	2,54	2,60
K2O	0,40	0,35	0,41	0,36	0,43	0,41	0,13	0,44	0,30	0,34	0,45
P2O5	0,27	0,27	0,28	0,28	0,29	0,28	0,27	0,31	0,34	0,34	0,30

1: Average bulk cumulate with 5 % granophyre
2: Average bulk cumulate with 2 % granophyre
3: Column 1 after subtraction of 5 % equilibrium olivine (Fo68)
4: Column 2 after subtraction of 5% equilibrium olivine (Fo68)
5: Column 3 after subtraction of 5% equilibrium plagioclase (An70).
6: Geikie Fm., GGU 98376, profile 47
7: Geikie Fm., GGU 98367, profile 47

9: Geikie Fm., GGU 98397, profile 48
10: Geikie Fm., GGU 98436, profile 51
11: Geikie Fm., GGU 98445, profile 51
12: Geikie Fm., GGU 98880, profile 76
13: Geikie Fm., GGU 98538, profile 55
14: Geikie Fm., GGU 98378, profile 47

The Skaergaard deposit

Exploration history

The potential for a precious metal deposit in the Skaergaard intrusion was first recognised in anomalous gold-bearing stream sediment samples from the river draining the northern side of Forbindelsesgletscher in the centre of the intrusion. Platinova Resources Ltd. and the Geological Survey of Greenland (GGU) conducted in the summer of 1986 a joint stream sediment sampling programme in the intrusion. The source of the gold was discussed and the consensus was reached that the most likely section in the intrusion for the origin of the gold was at the initiation of sulphur saturation in the magma at the major petrogenetic anomaly - the so called Triple Group - in the upper part of MZ. The Triple Group is a very marked macrorythmicly layered sequence that is easily identified all over the intrusion.

In 1987 an initial chip-line and drilling programme (portable GSC drill) was carried out and identified a mineralised zone within the upper 60 meters of MZ. A large chip line programme conducted in 1988 identified the mineralised horizon where ever the upper part of MZ is exposed in the intrusion. In 1989 11 drill holes (BQ; DHH 89-1 to DHH 89-9b) at 5 sites and a number of Winky Drill holes at a single locality were completed and substantiated the findings of the previous years. A mineralised zone up to 40 meters thick with an upper mineralised reef rich in gold (Platinova reef, maximum values of 4-5 g/t over 1 metre) and a lower mineralised reef up to 12 meters thick characterised by palladium was identified. The palladium-rich horizon is mostly several meters thick and the concentrations generally reach 2-3 g/t palladium, but concentrations up to 5 g/t over 1 meter are also observed. The palladium enrichment can be up to 7 m wide at a cut off of 1 g/t palladium. Palladium concentrations decrease slowly over c. 10 meters below the Pd level to less than 0.1 g/t. In all cases the palladium-rich horizon is located at the plagioclase-rich macrorythmic layer defined as L0 (L zero) (Fig. 8).

A 5 month drilling campaign in 1990 supported all previous observations. The mineralisation is present in all parts of the intrusion though with the most elevated gold concentration towards the centre. I the late 80´s and the beginning of the 90´s the emphasis was on gold with prices in the range 400 US $/oz and little attention was paid to the palladium content. Palladium varied in value from 50 to 90 US $/oz. A reason for low interest in the palladium-rich part was also the apparently non-systematic variation in the stratigraphic position of the palladium-bearing horizon relative to the gold-bearing reef.
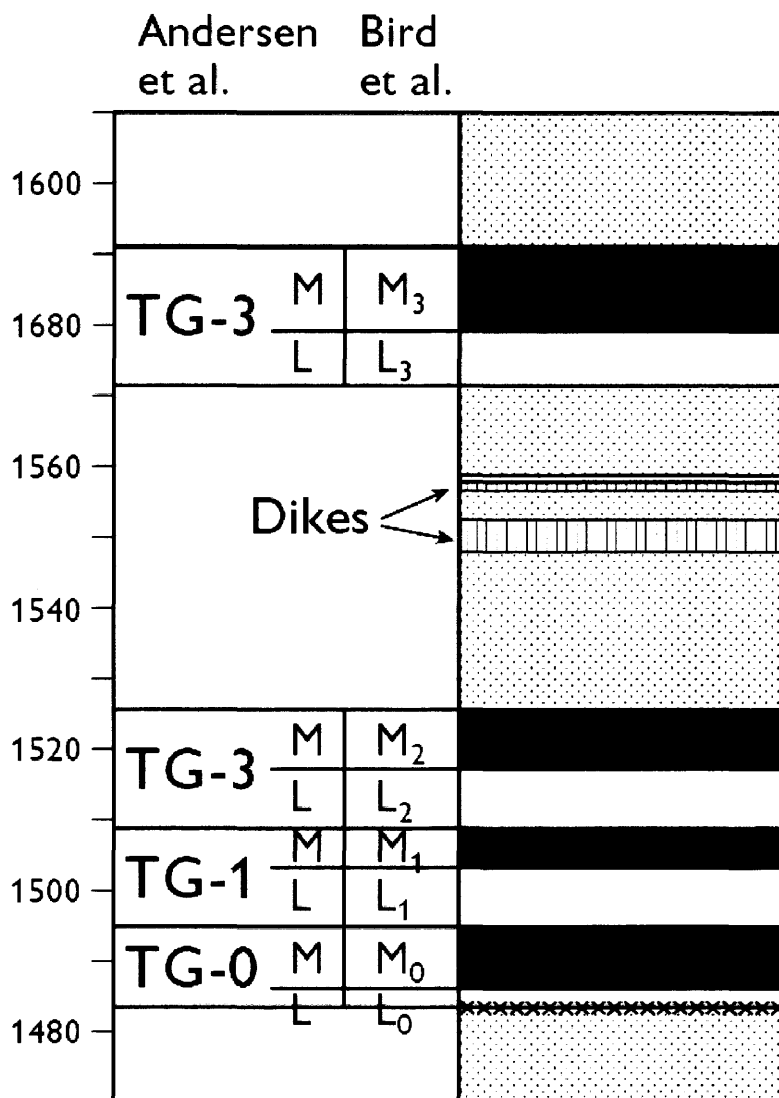
Figure 8. *Stratigraphy in the upper part of Middle Zone (MZ). Terminology from Andersen et al. (1998) and Bird et al. (1991). Lithological column to the right. White: leucogabbro; dotted: average gabbro; black: melanogabbro; vertical ruling: dykes. The Pd5-level of the deposit is located at L0 and marked with xxxxxxx. After Andersen et al. (1998)*

All cores were logged and stored in Sødalen, a valley 12 km to the east of the intrusion were a STOL dirt strip up to 700 m long was constructed. Selected sections of the core were transported to Canada for further investigation. In 1993 the Geological Survey of Greenland (GGU, since 1995 merged with the Geological Survey of Denmark to form the Geological Survey of Denmark and Greenland, GEUS) collected samples at 1 meter intervals throughout the mineralisation from 13 out of the total of 33 cores for research purposes. In the summer of year 2000 five up to 1100 m long cores were air lifted to Copenhagen for research purposes together with a selection of sections with specific scientific interest. They will be available for study in 2001. In addition cores intersecting the mineralised horizon from all drill sites have been selected, packed and shipped for storage in the core farm of the Bureau of Mineral and Petroleum in Kangerlussuaq, West Greenland.

During exploration the mineralised parts of the core were halved and quartered and samples, generally covering 1 meter of core were send for analyses. The many thousands of analyses and the core logs are summed up in great detail in the reports of Watts, Griffis and McOuat (1991). This is the material that forms the basis for the new descriptions and the re-interpretation of the structure and inventory of the deposit and the evaluation of the palladium potential of the Skaergaard intrusion.

Structure of the Skaergaard deposit

The deposit shows remarkable systematics. As shown in figure 9, the three drill cores - DDH 89-8, DDH 89-9 and DDH 90-18 - covering a lateral distance of c. 3 km in the intrusion contain palladium peaks that are readily correlated. Not only do the peaks show the same patterns in detail, they are also located at the same stratigraphic level relative to the magmatic layering in the gabbros of the intrusion. The main palladium concentration in the lower palladium peak which is conventionally referred to as the Pd2 peak, but in the detailed stratigraphy of the present report referred to as Pd5. Pd5 is located in the lower part of the plagioclase-rich macrorythmic layer L0 and the melanocratic gabbros just below. The L0 layer can be located throughout the intrusion visually and by density measurements. The global resource described below is contained in the c. 5 meters of gabbro below the density minimum in the L0 macrorythmic plagioclase-rich gabbro. The peak concentration of palladium is located app. 2 meters below the density minimum in L0. This correlation is confirmed in all 8 cores for which detailed density information is available (Table 4). Due to the sagging of the magmatic layering in the centre of the intrusion, the Pd5 mineralised level has a bowl shape.

Distinct palladium peaks can be identified above Pd5. The number of developed peaks depends on the location of the drill core. Figures 10 shows the variation in a selection of chip lines and drill cores in an E-W cross section and a N-S section from the northern part of the intrusion to the south central part of the intrusion. An increasing number of mineralised levels is developed over Pd5 from rim to centre of the intrusion and as shown in figure 9 the additional Pd-levels are identified as Pd4b, Pd4a, Pd3b, Pd3a, Pd2b, Pd2a, Pd1/Au1, Au2, and so on to at least Au4.
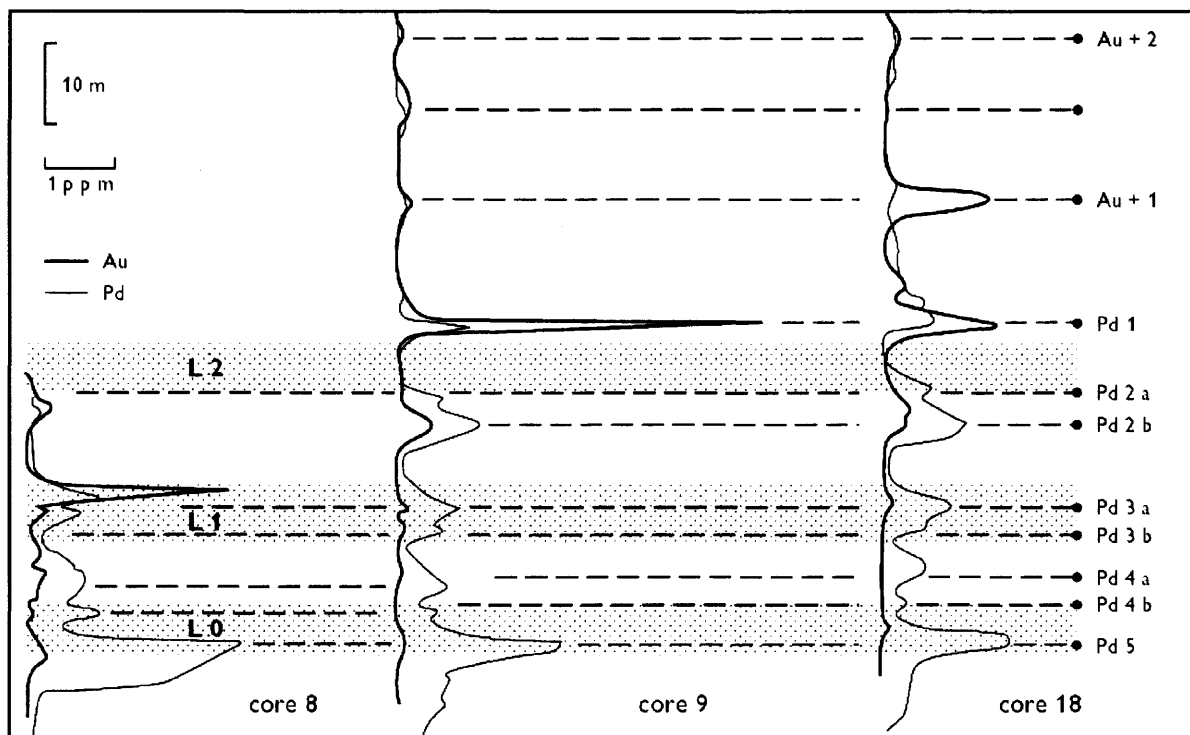
Figure 9. *Correlation of mineralisation anomalies in DDH 89-8, DDH 89-9 and DDH 90-18. Data from Watts, Griffis and McOuat (1991).*

Table 4. *Correlation between density interval and interval with Pd > 1g/t in the Pd5 level. Depth in drill cores in meters.*

DHH	density		chemistry	
	density minimum in L0	density indicated base of L0	top of Pd5 anomaly at 1 g/t Pd cut off	base of Pd5 anomaly at 1 g/t Pd cut off
89-02	202	207	201	206
89-09	485	488	484	488
90-13	469	472	469	474
90-14	192	195	192	199
80-18	1010	1014	1010	1013
90-22	1031	1036	1031	1036
90-23A	805	810	806	811
90-24	1055	1060	1055	1060
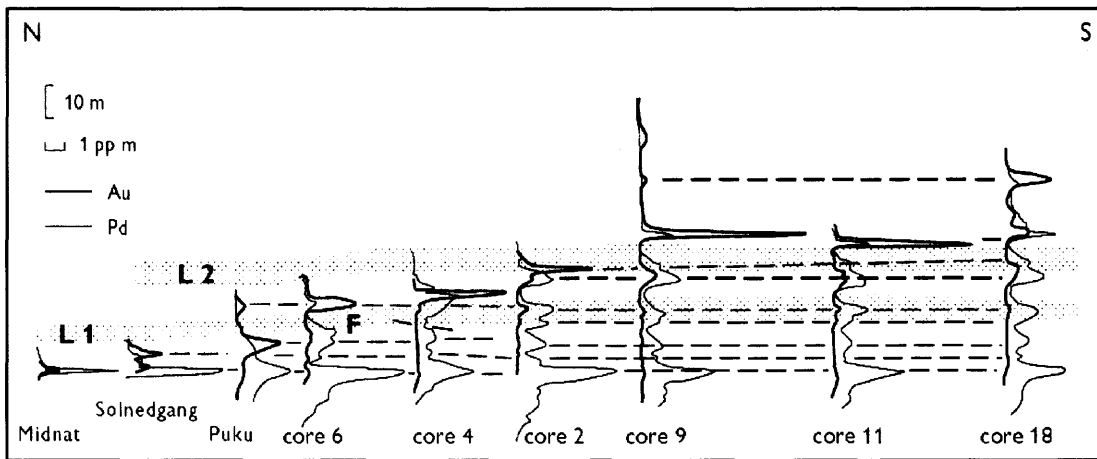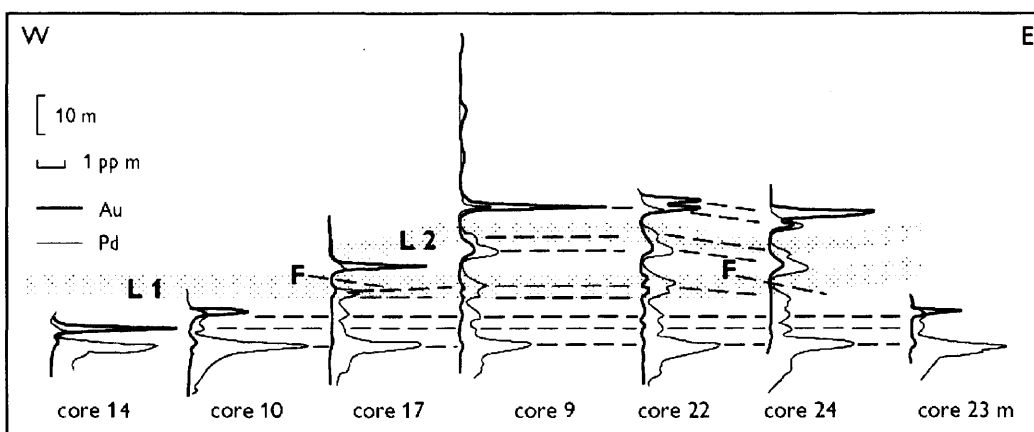
Figure 10. *Correlation of palladium and gold anomalies: (a) N-S section: (b) E-W section. Data from Watts, Griffis and McOuat (1991).*

The mineralised levels are always present at constant relative stratigraphic height and this systematic pattern appears to hold throughout the intrusion. It is remarkable that cores near the margin of the intrusion, in which only the lower mineralised levels – e. g. Pd5 and Pd4 - are developed, still show small palladium peaks at the levels where Pd3, Pd2 and Pd1 is developed in the more centrally located cores. This indicates that the mineralised levels exist whether there are precious metal concentrations in the melt available to fill them, or not, and that the structure of the deposit is controlled by the crystallisation of the gabbros. In every core the main gold concentrations is located in the uppermost filled palladium level or in a gold dominated level above (e. g., DHH 90-18). This applies to the entire mineralisation without known exception.

The structural systematics of the mineralisation are paralleled by chemistry. The 10-12 metres of mineralised gabbro below the peak value of the Pd5 level shows in a series of cores
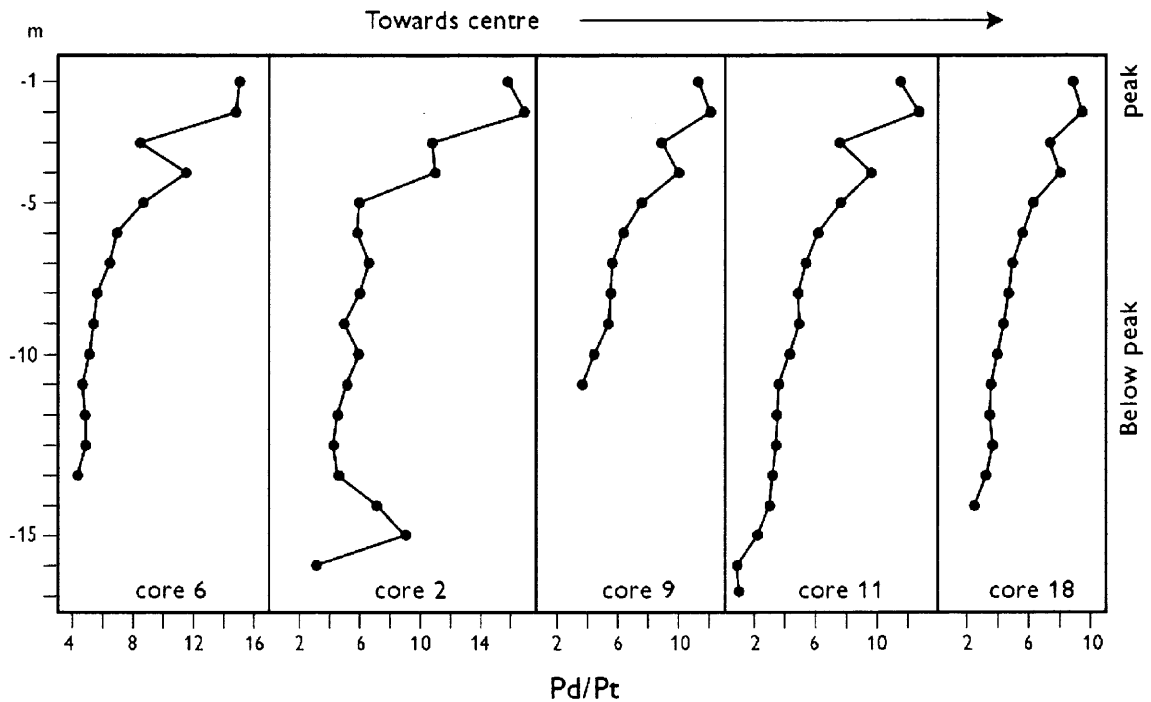
Figure 11. *Pd/Pt ratio variation in Pd5-level. Data from Watts, Griffis and McOuat (1991)S (see also Andersen et al., 1998).*

from rim to centre of the intrusion a general decrease in Pd/Pt ratio and a correlated development in Pd/Pt ratios (Fig. 11).

Close to the margin of the intrusion no other mineralised level is developed and the Pd5 level hosts the main Pd concentration as well as the main gold concentration. In a cross section the Pd5 level thus shows a systematic variation from a centre relatively enriched in Pt (the Pt/Pd is only 0.1), increasing Pd/Pt ratio and increasing total palladium concentrations away from the centre to a rim enriched in gold. This variation can be visualised as a gold-rimmed palladium bowl comparatively enriched in platinum in the centre. All the mineralised levels show this internal variation and can be pictured as a stack of gold-rimmed bowls of decreasing size with decreasing Pt/Pd up through the stack and from centre to rim of the individual bowl (Fig. 12). Such a district structural and chemical control strongly suggests fundamental magmatic control of the mineralisation process.
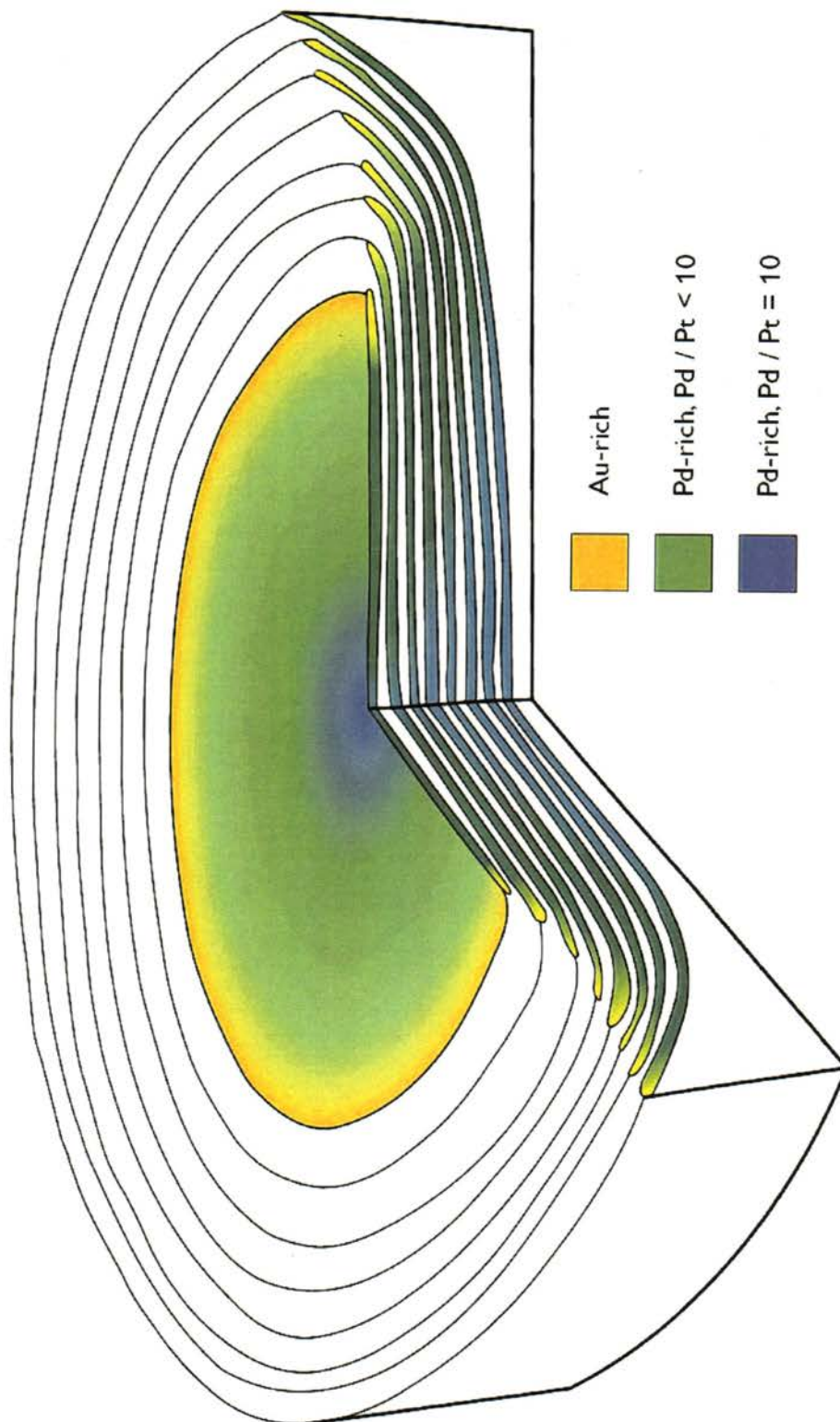
Figure 12. *Model for mineralisation based on drill core and chip line data. Not to scale. Vertical scale ca. 60 m, diameter 7 km. Au-rich up to 4 g/t over 1 m: Pd up to 5 g/t over 1 m and "Pt-rich" up to 3 g/t Pd with Pd/Pt equal to 10.*

Mineralogy of the deposit

The marked systematics in the chemistry of the deposit suggests a strong mineralogical control on the bulk concentrations Au and PGM. Mineralogical investigations of Au and PGM phases are in progress and the information below is preliminary.

Sulphide mineralogy

Three phases are common trough out the mineralisation:

Digenite: Cu_9S_5
Bornite: Cu_5FeS_4
Chalcopyrite: $CuFeS_2$

The reader is referred to Bird *et al.* (1991), Arnasson & Bird (1995) and Andersen *et al.* (1998) for more detailed petrographic information.

Precious metal mineralogy

Preliminary descriptions of the mineralogy and petrography of the precious metal phases and related sulphides are found in Bird *et al.* (1991), Arnasson & Bird (1995), Andersen *et al.* (1998), Rasmussen, Andersen & Nielsen (1997) and from unpublished EMP analyses. In the Pd5 level the precious metal form alloys of copper, gold and palladium and a suite of precious metal arsenites, sulphides and tellurrides. The modal proportions between the different phases in the different parts of the deposit have not been determined. Many mineralogical species have not yet been named and determined from the EMP analyses and the structural formulae are often provisional.

In some cases the alloys form crystals trapped in the rims of silicate cumulus crystals, but mostly in intercumulus parageneses and in immiscible sulphide droplets. In a few cases crystals of precious metal alloys can be seen to have dropped out of droplet of sulphide melt. lit appears that the precious metal alloys are liquidus phases in immiscible sulphide droplets formed in response to sulphur saturation in the intercumulus melt.

In the central part of the intrusion (DDH 90-18, and DDH 90-24) the Pd5-level seems characterised by:

CuPd alloys:	(Cu,Fe)(Au,Pd,Pt) showing a significant variation in Cu/Pd from 2 to 0.5 and variable contents of Au, Fe, Sn and Pt including CuPt.
Keithconnite:	$Pd_{3-x}(As,Te)$
Vysotskite:	PdS
Kotulskite:	PdTe
Hongshiite:	CuPt

Closer to the margin of the intrusion (DDh 90-14 and DDH 90-23A) the Pd5-level seems characterised by:

CuPd alloys: $(Cu,Fe)(Au,Pd,Pt)$ showing a significant variation in Cu/Pd from 2 to 0.5 and variable contents of Au, Fe, Sn, Te and Pt including CuPt.

Keithconnite: $Pd_{3-x}(As,Te)$

Pd_4As

The potential for a platinum reef

Systematic analyses of Pt and Pd up through the gabbros of the intrusions show a major shift in the Pd/Pt ratio at a level app. 150 m below the identified Pd5-level (Nielsen *et al.*, 1996). The ratio changes from 3/1 to *c.* 10/1. It is not found likely that the change in the ratio reflects addition of palladium, but rather the loss of platinum that potentially could be concentrated in a mineralised horizon. The gabbros below the Pd5-level have not been chipped or investigated for potential mineralisations and it is suggested that the succession below the Pd5 peak, especially app. 120 to 170 m below the Pd5 peak should be investigated.

Evaluation of the potential of the mineralisation

The evaluation of the palladium potential in the Skaergaard intrusion is entirely based on the observations in the intrusion.

The drill cores from the intrusion give information on the concentrations of the precious metals at 0.5-1.0 km intervals over a large area and although the distances are significant the continuity, and the systematics of the mineralisation suggests that the data can be used for calculation of the potential. A contributing factor is that the re-chipping of exploration profiles and calculation of 1 m average concentrations in three passes on the same core give precious metal concentrations within an uncertainty of 10 rel. % (e. g., Nielsen, 1989). This suggests a very well controlled mineralisation and supports that extrapolation between drill cores is permissible.

Note should be made that a more detail investigation of many of the drill cores and a significant increase in the aerial coverage of the large areas, especially in the eastern part of the intrusion, will increase the statistics and the certainty with which the potential can be evaluated.

The resource potential

The potential global resource in the Pd5-level of the mineralisations (Table 5) is calculated based on a cut off of 1 g/t palladium. The volume has been calculated from average widths of gabbro with > 1 g/t palladium and the area of the intrusion believed and/or confirmed to host the Pd5 level and the average concentration in the intersects with >1 g/t palladium in all drill cores. The density is measured and calculated to 3.15 − 3.20 in the lower part of the Pd5-level. The area is estimated to app. 19 km^2, the average thickness of the ore zone to 4.7 meters and the average palladium content of 1.9 g/t. In total this gives a potential for 285 million tons over 4.7 meters with a total of ca. 17 million oz palladium. The combined palladium, platinum and gold varies dependent on the preferred width of the mineralisation and reach in Pd5 > 5 g/t over 1 m.

Concentrations in 2 m sections

The tonnage in the most palladium rich part of the Pd5-level is calculated based on 2 meter averages. Based on a systematic record of the analytical values in exploration reports all the best 2 meter intersects are compiled. It is evaluated that an area of c. 10 km^2 in the west central part of the intrusion contains 2.4 g/t palladium and a total of > 4.6 million oz palladium. In total this resource would amount to >60 million tons (Table 6).

Table 5. *Ressource potential evaluation. See text for explanation.*

Average for 280 million tons over 4,7 m (average)[1]
19 square km; density 3,20

DDH	width (m)	Au ppm	Pd ppm	Pt ppm	combinded
average 89/1-2	5,0	0,06	2,09	0,17	2,32
average 89/3-4	4,5	0,09	1,60	0,17	1,86
average 89/5-6	4,0	0,09	2,24	0,17	2,50
average 89/7-8	7,0	0,14	2,13	0,16	2,43
average 89/9	6,6	0,09	1,85	0,19	2,13
90/10 Pd5	4,6	0,15	2,40	0,12	2,67
90/11 Pd5	4,0	0,09	1,55	0,14	1,78
90/12 Pd5	5,0	0,09	1,76	0,10	1,95
90/13 Pd5	3,0	0,09	1,73	0,15	1,97
90/14 Pd 5	6,0	0,09	1,82	0,12	2,03
90/17A Pd5	4,0	0,06	1,93	0,17	2,16
90/18 Pd5	3,0	0,09	1,58	0,19	1,86
90/19 Pd5	3,0	0,13	1,64	0,15	1,92
90/22 Pd5	5,0	0,08	1,83	0,18	2,09
90/23 Pd5	5,0	0,10	1,96	0,11	2,17
90/23A Pd5	5,0	0,12	1,86	0,12	2,10
90/24 Pd5	5,0	0,07	1,76	0,15	1,98
Average	**4,69**	**0,10**	**1,87**	**0,15**	**2,11**

Average for 120 million tons over 2 m[1]
19 square km; density 3,20

DDH	width (m)	Au ppm	Pd ppm	Pt ppm	combinded
average 89/1-2	2,00	0,07	2,78	0,20	3,05
average 89/3-4	2,00	0,09	1,87	0,19	2,15
average 89/5-6	2,00	0,10	2,75	0,19	3,04
average 89/7-8	2,00	0,24	2,84	0,23	3,31
average 89/9	2,00	0,10	2,90	0,24	3,24
90/10 Pd5	2,00	0,20	3,40	0,14	3,74
90/11 Pd5	2,00	0,11	1,91	0,15	2,17
90/12 Pd5	2,00	0,12	2,48	0,12	2,72
90/13 Pd 5	2,00	0,09	1,88	0,16	2,13
90/14 Pd 5	2,00	0,10	2,90	0,17	3,17
90/17A Pd5	2,00	0,08	2,55	0,19	2,82
90/18 Pd5	2,00	0,11	1,76	0,20	2,07
90/19 Pd5	2,00	0,12	1,90	0,17	2,19
90/22 Pd5	2,00	0,10	2,31	0,17	2,58
90/23 Pd5	2,00	0,13	2,45	0,12	2,70
90/23A Pd5	2,00	0,16	2,55	0,13	2,84
90/24 Pd5	2,00	0,10	2,40	0,18	2,68
	2,00	**0,12**	**2,45**	**0,17**	**2,74**

1: only cores with full recovery included.

Table 6. *Summary of drill core and chip line information. Data from Watts, Griffis and McOaut, 1991).*

BQ drill core	interval m	width m	Au ppm	Pd ppm	Pt ppm	combined g/t
89/2	202-204	2,0	0,07	2,78	0,20	3,06
89/2	202-203,4	1,4	0,08	2,90	0,21	3,19
89/2	201-206	5,0	0,06	2,09	0,17	2,32
89/3	256-258	2.0	0,08	2,12	0,18	2,38
89/3	255-258	3,0	0,11	2,00	0,18	2,29
89/3	255-259	4,0	0,10	1,82	0,17	2,09
89/4	273-275	2,0	0,10	1,62	0,19	1,91
89/4	273-277	4,0	0,07	1,37	0,17	1,61
89/4	274-275	1,0	0,10	1,78	0,22	2,10
89/5	165-167	2,0	0,09	2,75	0,18	3,02
89/5	164-168	4,0	0,08	2,32	0,17	2,57
89/6	160-162	2,0	0,10	2,75	0,19	3,04
89/6	159-163	4,0	0,09	2,15	0,17	2,41
89/7	86-87	1,0	0,23	3,15	0,29	3,67
89/7	85-87	2,0	0,25	3,07	0,26	3,58
89/7	87-88	1,0	0,26	3,08	0,26	3,60
89/7	84-91	7,0	0,15	2,18	0,17	2,50
89/8	85-87	2,0	0,22	2,60	0,20	3,02
89/8	85-88	3,0	0,23	2,49	0,17	2,89
89/8	84-91	7,0	0,13	2,07	0,15	2,35
89/9	485-487	2,0	0,10	2,07	0,18	2,35
89/9	484-488	4,0	0,09	1,68	0,16	1,93
89/9A	485-486	1,0	0,15	5,10	0,42	5,67
89/9A	485-487	2,0	0,10	4,40	0,35	4,85
89/9A	482-494	12,0	0,05	2,10	0,24	2,39
89/9B	484-486	2,0	0,10	2,23	0,19	2,52
89/9B	483-487	4,0	0,13	1,78	0,17	2,08
90/10	443,2-445,2	2,0	0,20	3,40	0,14	3,74
90/10	443,4-445,0	1,6	0,20	3,51	0,14	3,85
90/10	443,6-444,6	1,0	0,23	3,85	0,14	4,22
90/10	442,6-447,2	4,6	0,15	2,40	0,12	2,67
90/11	676,7-678,1	1,4	0,13	2,12	0,15	2,40
90/11	676,5-678,5	2.0	0,11	1,91	0,15	2,17
90/11	675,7-679,7	4,0	0,09	1,55	0,14	1,78
90/12	634-636	2,0	0,12	2,48	0,12	2,72
90/12	633-638	5,0	0,09	1,76	0,10	1,95
90/13	470-471	1,0	0,12	1,96	0,18	2,26
90/13	470-472	2,0	0,09	1,88	0,16	2,13
90/13	469-472	3,0	0,09	1,73	0,15	1,97
90/14	194-196	2,0	0,10	2,90	0,17	3,17
90/14	194-195	1,0	0,14	3,18	0,16	3,48
90/14	193-199	6,0	0,09	1,82	0,12	2,03
90/17A	499-501	2,0	0,08	2,55	0,19	2,82
90/17A	498-502	4,0	0,06	1,93	0,17	2,16
90/18	1010-1012	2,0	0,11	1,76	0,20	2,07
90/18	1010-1013	3,0	0,09	1,58	0,19	1,86
90/19	589-592	3,0	0,13	1,64	0,15	1,92
90/19	590-592	2,0	0,12	1,90	0,17	2,19

Core no	interval m	width m	Au ppm	Pd ppm	Pt ppm	combined g/t
90/20	976-978	2,0	0,11	1,25	0,21	1,57
90/22	1032-1034	2,0	0,10	2,31	0,17	2,58
90/22	1031-1036	5,0	0,08	1,83	0,18	2,09
90/23	810-815	5,0	0,10	1,96	0,11	2,17
90/23	811-813	2,0	0,13	2,45	0,12	2,70
90/23A	807-809	2,0	0,16	2,55	0,13	2,84
90/23A	806-811	5,0	0,12	1,86	0,12	2,10
90/23A	1055-1060	5,0	0,07	1,76	0,15	1,98
90/24	1056-1058	2,0	0,10	2,40	0,18	2,68
90/25A	369-370,45	1,5	0,09	2,40	0,17	2,66

Pack sack drill

Puku P3	2,00-4,50	2,50	1,30	0,74	0,42	2,46

Chip line

gabbrogletscher	chip line	9,40	0,08	1,25	0,11	1,44
gabbrogletscher	chip line	4,73	0,15	1,30	0,11	1,56
middag but	chip line	5,21	0,35	1,73	0,12	2,20
midnat ridge	chip line	1,91	0,15	1,40	0,14	1,69
dru couloir	chip line	4,13	0,18	1,70	0,15	2,03
Solskin, r.c.	chip line	4,44	0,26	1,07	0,13	1,46
solnedgangs blv	chip line	2,16	0,27	1,60	0,13	2,00
peppermint	chip line	3,73	0,16	1,50	0,10	1,76
Forbindelse	chip line	1,60	0,21	2,50	0,20	2,91
Pukku N	chip line	3,26	0,25	1,60	0,13	1,98
Lille Mellemø	chip line	2,93	0,40	1,30	0,09	1,79
Hate and Discontent	chip line	3,17	0,42	1,30	0,13	1,85
Les Courtes	chip line	3,96	0,31	1,20	0,10	1,61
Ladakh	chip line	8,82	0,11	1,45	0,12	1,68
Ladakh	chip line	4,41	0,20	1,60	0,09	1,89
MacWager	chip line	4,81	1,70	1,90	0,16	3,76
MacWager	chip line	9,62	0,86	1,50	0,15	2,51
Bellevue	chip line	2,55	0,20	2,00	0,16	2,36
middag r,c,	chip line	2,00	0,72	2,37	0,15	3,24
Dru Couloir r,c,	chip line	2,00	0,61	2,16	0,15	2,92
Solnedgangs r,c,	chip line	1,68	0,64	1,93	0,15	2,72
Solnedgangs r,c,	chip line	1,26	0,65	2,23	0,18	3,06
Solnedgangs	chip line	3,48	0,32	1,65	0,12	2,09
Puku AA	chip line	1,45	1,50	0,41	0,03	1,94
Bjørneskin r.c. *	chip line	1,18	1,04	1,70	0,17	2,91

Maximum width

The greatest width in the Pd5 level at a cut off at 1 g/t palladium is found in the areas on the north side and below Forbindelsesgletscher (e g., DHH 89-1, 2, 5, 6, 7 and 8). The width is up to 7 m (DDH 89-7 and 8) and the tonnage may be as high as 25-30 million tons (>20 million tons) with 2.2 g/t palladium and a total of 1.4 million oz palladium over an average width of >5 m (Table 6). Only few drill cores and a limited number of chip lines are available from this area, but the potential appear to be present.

Technical aspects

The evaluation of the potential is dependent on a number of technical aspects including the recovery of the metals, grade control, the orientation of the mineralised horizon, etc. Recovery tests carried out by Lakefield Research for Platinova Resources Ltd. suggest that a recovery of 90 % is obtainable (Lakefield, 1988 and 1989). The tests were carried out on the Au-dominated ore composed of Cu-Au alloys using fine crushing and flotation. No cyanidation was suggested. It is here assumed that a similar recovery could be obtained for the Cu-Pd alloys of the Pd5-level. What the recovery would be in the more marginal PdxAs characterised parts of the Pd5-level is unknown.

The mineralisation is not visible by naked eye and the mineralisation would probably be almost impossible to locate visually underground. The fate of the Hartley mine in Great Dyke in Zimbabwe clearly demonstrates that grade control is a major issue. An exploitation of the Skaergaard deposit would thus require development of grade control technology and methods. Several aspects of the mineralisation, however, suggests that this would be possible. The strong structural, geochemical and petrogenetic control may give possibilities for a grade control using the primary magmatic density variation, mineralogical variation and/or chemical layering in the very well controlled mineralisation.

As noted above densities have been measured up through the mineralised zone at 0.5 or 1 meter intervals in 13 drill cores and show that the cores can be correlated in great detail. This suggests that the individual magmatic layers in the intrusion do not vary significantly throughout the investigated area and that the internal density variation can be used for a fairly exact identification of the stratigraphic levels. It seems more than likely that the global resource of 2 g/t palladium in a width of 4.7 m can be recovered by mining the 4.7 m of gabbro below the density minima in the plagioclase rich layer in the L0 macrorythmic sequence. In no case has the correlation failed and the easily identified density minima in L0 is a fixed marker relative to the palladium mineralisation in Pd5.

Summary

The available information on the Skaergaard intrusion precious metal mineralisation can be summed up as follows:

1. The mineralisation in the Skaergaard intrusion is world class palladium mineralisation.

2. The mineralisation is stratigraphically well controlled and located in the upper 60 m of the Middle Zone of the intrusion.

3. Marker horizons allow the mineralisation to be easily and precisely located by density measurements and petrography.

4. The mineralisation consist of a series of very well defined mineralised levels in a structure best described as a stack of gold-rimmed bowls defined by palladium. The bowls decrease in size upwards.

5. The lowest mineralised level the Pd5 level has a potential for 285 million tons of ore with 1.9 g/t palladium over an average width of 4.7 meters in an area of $c.$ 19 km^2; a potential for >60 million tons with 2.4 g/t palladium over 2 meters in an area of >10 km^2 and a potential for 25 – 30 million tons with 2.2 g/t palladium over >5 meters. No other mineralised level is known to contain palladium concentrations > 1 g/t in any extended volumes.

6. The precious metals generally occur as Cu-Pd alloys and Pd arsenites in subhedral to euhedral crystals in the intercumulus matrix or in adhedcumulus rims on liquidus phases.

7. Recoveries of Cu-Au alloys from the gold-bearing rims of the bowls by floatation reach up to 92 % and similar recoveries could be expected for Cu-Pd alloys from the palladium mineralisation.

8. The ore in the Pd5-level contains besides palladium, platinum in the ration Pd/Pt = $c.$ 10, minor gold, copper, tin and elements related to ilmenite and magnetite.

9. The density in the ore horizon is $c.$ 3.15 – 3.2.

10. The Skaergaard intrusion is located at tide water in an alpine terrain on the South-East Greenland coast in an area with no permafrost.

11. The geothermal gradient is $c.$ 25°C/km.

12. Flight time from Northwest Iceland is ca. 1.5 hours.

13. The coastal waters of East Greenland are navigable by ice class vessels from July to October. Transit time from Iceland is app. 20 hours at ca. 10 knots.

References

Andersen. J.C.O., Rasmussen, H., Nielsen, T.F.D. & Rønsbo, J.G. 1998: The triple group and the Platinova reefs in the Skaergaard intrusion: stratigraphic and petrographic relations. Economic Geology **93**, 488-509.

Arnasson, J.G. & Bird, D.K. 1995. Palladium minerals from the Skaergaard intrusion, East Greenland. Transactions of the American Geophysical Union **76**, F641 only.

Bird, D.K., Brooks, C.K., Gannicott, R.A. & Turner, P.A. 1991: A gold-bearing horizon in the Skaergaard intrusion, East Greenland. Economic Geology **86**, 1083-1092.

Brooks, C.K. 1968: On the distribution of zirconium and hafnium in the Skaergaard intrusion, East Greenland. Geochem et Cosmochem Acta **33**, 357-374.

Deer, W.A., Howie, R.A. & Zussman, J. 1966: An introduction to the rock-forming minerals. 528 pp. London: Longman.

Geodætisk Institut 1975: Skærgården 1:20 000. København: Kort og Matrikelstyrelsen.

Hirschmann, M., Renne, P.R. & McBirney, A.R. 1997: ^{40}Ar/^{39}Ar dating of the Skaergaard intrusion. Earth and Planetary Science Letters **146**, 645-658.

Hunter, R.H. & Sparks, R.S.J. 1987: The differentiation of the Skaergaard intrusion. Contributions to Mineralogy and Petrology **95**, 451-461.

Irvine, N.T. 1992: Emplacement of the Skaergaard intrusion. Carnegie Institution of Washington Year Book **91**, 91-96.

Irvine, N.T., Andersen, J.C.Ø. & Brooks, C.K. 1998: Included blocks (and blocks within blocks) in the Skaergaard intrusion: Geological relations and the origins of rythmic modally graded layers. Geological Society of America Bulletin **110**, 1398-1447.

Lakefield Research 1988: The recovery of gold, progress report No. 2. 29 pp. Unpublished report, Lakefield Research, Canada (in archives of the Geological Survey of Denmark and Greenland, GEUS Report File 20918).

Lakefield Research 1989: The recovery of gold, progress report No. 1. 41 pp. Unpublished report, Lakefield Research, Canada (in archives of the Geological Survey of Denmark and Greenland, GEUS Report File 20920)

Larsen, L.M., Watt, W.S. & Watt, M. 1989: Geology and petrology of the Lower Tertiary plateau basalts of the Scoresby Sund region, East Greenland. Bulletin Grønlands Geologiske Undersøgelse **157**, 149 pp.

McBirney, A.R. 1989a: Geological map of the Skaergaard intrusion, East Greenland. 1:20 000. Eugene: Department of Geology, University of Oregon

McBirney, A.R. 1989b: The Skaergaard layered series:1, Structure and average compositions. Journal of Petrology **30**, 363-397.

McBirney, A.R. 1996: The Skaergaard intrusion. In Cawthorn, R.G., ed., Layered Intrusions (Developments in Petrology **15**). Amsterdam, Elsevier,147-180.

Maaløe, S. 1976: The zoned plagioclase of the Skaergaard intrusiom. Journal of Petrology **17**, 318-419.

Nielsen, T.F.D. 1987: The Tertiary alkaline magmatism in East Greenland: A review. In: Fitton, J.,G. & Upton, B.G.J. (eds): Alkaline igneous rocks. Geological Society of London Special Volume **30**, 489-515.

Nielsen, T.F.D. 1989: Gold mineralisation in the Skaergaard intrusion. Open file series **89/7** Grønlands Geologiske Undersøgelse 14 pp.

Nielsen T.F.N. & Andersen, J.C,Ø 1996: 3-D model for the Skaergaard intrusion, its internal structure, volume relations and Au-Pd mineralisation. Transactions of the American Geophysical Union EOS 77, **46**, 823 only.

Norton, D., Taylor, H.P. & Bird, D.K. 1984: The geometry and high temperature brittle deformation of the Skaergaard intrusion. Journal of Geophysical Research **89**, 10178-10192.

Rasmussen, H., Andersen, J.C.Ø & Nielsen, T.F.N 1997. Composition and variation of sulphide and precious metal phases in the Au and PGE mineralization of the Skaergaard Intrusion, East Greenland. EUG 9, March 1997. Terra Abstracts **9**, Abstract Supplement 1.

Thy, P., Brooks, C.K., Lesher, C.E. & Nielsen, T.F.D. & 1996. Eksperimental modeling of Skaergaard cumulates. Transactions of the American Geophysical Union 1996 Fall meeting, EOS **77**, 46, F822.

Wager, L.R. & Brown, G.M. 1968: Layered igneous rocks. Edinburgh, Oliver and Boyd, 558 p.

Wager, L.R. and Deer, W.A. 1939: Geological investigations in East Greenland:, Part III, The petrology of the Skaergaard intrusion, Kangerdlugssuaq, East Greenland. Meddelelser om Grønland **105** (4), 1-346.

Watts, Griffis & McOuat 1991: The Skaergaard project, Platinova/Corona concession, East Greenland 2A, 71-165. Unpublished report, Watts, Griffis & McOuat, Toronto, Canada (in archives of the Geological Survey of Denmark and Greenland, Report File 20848).